

will be published in Journal of Applied Physics

# Wave excitations of drifting two-dimensional electron gas under strong inelastic scattering

V. V. Korotyeyev, V. A. Kochelap

*Department of Theoretical Physics, Institute for Semiconductor Physics,  
Pr. Nauki 41, Kiev 03028, Ukraine*

L. Varani

*Institut d'Électronique du Sud, CNRS UMR 5214, University Montpellier 2 France*

## Abstract

We have analyzed low-temperature behavior of two-dimensional electron gas in polar heterostructures subjected to a high electric field. When the optical phonon emission is the fastest relaxation process, we have found existence of collective wave-like excitations of the electrons. These wave-like excitations are periodic in time oscillations of the electrons in both real and momentum spaces. The excitation spectra are of multi-branch character with considerable spatial dispersion. There are one acoustic-type and a number of optical-type branches of the spectra. Their small damping is caused by quasi-elastic scattering of the electrons and formation of relevant space charge. Also there exist waves with zero frequency and finite spatial periods - the standing waves. The found excitations of the electron gas can be interpreted as synchronous in time and real space manifestation of well-known optical-phonon-transient-time-resonance. Estimates of parameters of the excitations for two polar heterostructures, GaN/AlGaIn and ZnO/MgZnO, have shown that excitation frequencies are in THz-frequency range, while standing wave periods are in sub-micrometer region.

PACS numbers: 72.30.+q, 72.20.Ht, 73.63.Hs

## I. INTRODUCTION

In semiconductor materials and heterostructures at low temperature, when  $e^{-\hbar\omega_0/k_B T} \ll 1$  ( $\omega_0$ ,  $k_B$  and  $T$  are the optical phonon frequency, the Boltzmann constant and the temperature, respectively) the absorption of optical phonons by electrons is practically absent. While optical phonon emission can be the dominant scattering mechanism for hot electrons if electron-optical phonon coupling is strong enough. In samples with high electron mobility, where the electrons undergo only weak quasi-elastic scattering at a low field, the dynamics of an electron subjected to a steady state high electric field  $F_0$  is the following. The electron is almost ballistically accelerated by the field until reaching the optical phonon energy. Then, the optical phonon emission occurs so that the electron loses practically all its energy and stops. The processes are repeated in time. This dynamics gives rise to temporal and spatial modulation of the electron momentum,  $\mathbf{p}$ , and velocity  $\mathbf{v}$  with characteristic time period,  $\tau_F = p_0/eF_0$ , and length,  $l_F = eF_0\tau_F^2/2m^* \equiv \hbar\omega_0/eF_0$ , where  $p_0 = \sqrt{2m^*\hbar\omega_0}$ ,  $e$  is the elementary charge and  $m^*$  is the electron effective mass.

For this kind of cyclic motion, the electron momentum space can be divided into two regions. The first is the *passive* region, where the electron energy  $E(\mathbf{p}) < \hbar\omega_0$ . In this region inelastic scattering by optical phonons is almost absent, so that electron scattering is practically elastic and can be characterized by an elastic scattering time,  $\tau_p$ . The second region is the *active* region,  $E(\mathbf{p}) > \hbar\omega_0$ , where optical phonon emission is the dominant process, i.e.

$$\tau_{op}^{em} \ll \tau_p, \quad (1)$$

with  $\tau_{op}^{em}$  being the optical phonon emission time. Pronounced cyclic motion is possible, when

$$\tau_{op}^{em} \ll \tau_F \leq \tau_p, \quad (2)$$

i.e., the time of flight of the electrons through the passive region is shorter than the scattering time, while penetration of the electrons into the active region,  $p - p_0 = \Delta p$ , is sufficiently small,

$$\Delta p \sim p_0 \frac{\tau_{op}^{em}}{\tau_F} \ll p_0. \quad (3)$$

Actually, the latter inequalities define a range of the electric fields, where this kind of periodic motion can occur. The critical electric field necessary for the onset of the cyclic electron

motion is estimated to be

$$F_{cr} = \frac{p_0}{e\tau_p}. \quad (4)$$

The presented scenario is essentially single electron physical picture valid at low or modest electron concentrations, when  $e$ - $e$  collisions do not destroy the cyclic motion.

The possibility of cyclic acceleration-stop electron dynamics due to strong inelastic scattering by optical phonons was predicted six decade ago by Shockley.<sup>1</sup> Experimental evidences of the *cyclic dynamics in real space* were found by analyzing low temperature I-V characteristics of short diodes made from different polar materials: InSb,<sup>2</sup> InGaAs,<sup>3</sup> GaAs,<sup>4</sup> and InP.<sup>5</sup> Tens of cycles were identified at low temperatures. Very recently, comprehensive Monte-Carlo simulations of electrically biased short InN and GaN diodes have demonstrated the formation of stationary one-dimensional gratings of electron concentration and velocity at nitrogen temperature.<sup>6,7</sup>

In time (frequency) domain, the cyclic dynamics gives rise to a resonance phenomenon at the transit-time frequency  $\omega_F = 2\pi/\tau_F$ , frequently called optical phonon transient time resonance (OPTTR). The OPTTR induces a number of interesting effects (for review see Refs. 8,9). The most important manifestation of this phenomenon is the possibility of microwave amplification and generation in the sub-THz and THz frequency regions. The microwave generation based on OPTTR phenomenon was observed experimentally in InP samples for the frequency range 50 to 300 GHz.<sup>10</sup> For other indicated above bulk-like materials, the OPTTR generation was studied theoretically in details.<sup>8,9</sup>

Discussed cyclic electron dynamics should be even more pronounced for low-dimensional electron systems. Indeed, for the latter the onset of the optical phonon emission is much sharper because of specific features of the density of low-dimensional states. For comparison, the optical phonon emission rate  $1/\tau_{op}^{em}$  in bulk crystals is proportional to  $\sqrt{E(\mathbf{p}) - \hbar\omega_0}$  ( $0 < E(\mathbf{p}) - \hbar\omega_0 \ll \hbar\omega_0$ ), while for two-dimensional carriers,  $1/\tau_{op}^{em} \propto \mathcal{H}[E(\mathbf{p}) - \hbar\omega_0]$ , where  $\mathcal{H}[x]$  is the Heaviside step-function. In addition to a sharper threshold of the optical phonon emission, high mobilities and, thus, quasiballistic motion at energies  $E(\mathbf{p}) < \hbar\omega_0$  can be easily achieved for low-dimensional electrons, while their concentration can be controlled to avoid  $e$ - $e$  scattering. These important qualitative conclusions are supported by papers,<sup>11-13</sup> where, by the example of GaN quantum well heterostructures, it was shown the preference of their use to reach the cyclic electron motion. Note that effects similar to OPTTR are predicted for novel one-dimensional nanostructures - carbon nanotubes.<sup>14</sup>

Summarizing this short review, one can conclude that the cyclic electron dynamics is a quite general low-temperature phenomenon characteristic of many polar materials and heterostructures subjected to an electric field. It is believed that the phenomenon may lead to different effects, the most representative of them are spatial grating of electron concentration and velocity in finite size diodes and OPTTR resonance in the time/frequency domain for bulk samples.

In this paper, by investigating the case of two-dimensional electrons, we show that under the conditions of the cyclic electron motion, a novel type of weakly damped excitations of drifting electron gas exists. These excitations, quite different from well known plasmons, are periodic in time and in real space oscillations (waves) of electron concentration and charge both synchronized with electron redistributions in the momentum space. Their frequency-wavevector relation has infinite number of continuous branches,  $\omega^k(q)$ , with  $q$  being the wave vector of excitations and  $k = 0, \pm 1, \pm 2, \dots$ . The excitation damping is especially weak or even absent, when the frequency and/or the wavevector are multiples of  $\omega_F$  and/or  $q_F = 2\pi/l_F$ , respectively. Particularly, for  $q$  multiple of  $q_F$  standing waves ( $\omega = 0$ ) without any damping appear.

## II. MODEL AND EQUATIONS

It is well established that, for conditions when the cyclic electron motion can occur, steady state and high frequency electron transport can be described by semiclassical Boltzmann transport equation (BTE) for the electron distribution function in the momentum space. Under conditions (2), the electron distribution is mainly grouped in the passive region and essentially elongated along the electric field (the so-called *streaming distribution*). The BTE can be solved numerically by Monte-Carlo simulations or analyzed analytically with the use of same approximations adequate to the physical picture. These approximations include: the Baraff approximation<sup>15</sup> to take into account the anisotropic part and setting to zero the isotropic part of the distribution function in the active region because of the short emission time  $\tau_{op}^{em}$  (see discussions in Refs. 16,17 for bulk materials, and in Refs. 11, for two-dimensional systems). In this paper we will use the analytical approach.

Consider a uniform two-dimensional electron gas confined in narrow quantum well layer at  $z = 0$  (the quantum well thickness is negligible in comparison with the characteristic

lengths under consideration). Introduce the reference frame with  $X, Y$ -axes in the plane of the quantum well layer and  $Z$ -axis perpendicular to this plane. The applied electric field is along the  $X$ -axis. Nonequilibrium electrons are described by the distribution function  $\Phi = \Phi(p_x, p_y, \mathbf{r}, t)$ , which is, generally, dependent on the momentum,  $\mathbf{p} = \{p_x, p_y\}$ , the coordinate,  $\mathbf{r} = \{x, y\}$ , and time,  $t$ . Let  $N$  be the areal electron concentration given by doping. Then we define the distribution function in such a way, that  $N\Phi(\mathbf{p}, \mathbf{r}, t)d\mathbf{p}d\mathbf{r}$  is the number of electrons in the phase-space elementary volume  $d\mathbf{p}d\mathbf{r}$  located at the phase-space point  $\{\mathbf{p}, \mathbf{r}\}$ . The BTE for  $\Phi$  is

$$\frac{\partial \Phi}{\partial t} + \frac{\mathbf{p}}{m^*} \frac{\partial \Phi}{\partial \mathbf{r}} - e\mathbf{F} \frac{\partial \Phi}{\partial \mathbf{p}} = \hat{L}_{el}\{\Phi\} + \hat{L}_{op}\{\Phi\}, \quad (5)$$

where the collision integrals  $\hat{L}_{el}\{\Phi\}$  and  $\hat{L}_{op}\{\Phi\}$  describe the quasielastic scattering and the inelastic scattering by optical phonons, respectively.

An excitation of the drifting nonequilibrium electron gas can be considered as a perturbation of the stationary distribution with appearance of an additional field. Thus, we present the distribution function and the field as stationary and perturbed contributions:  $\Phi = \Phi_0 + \tilde{\Phi}$  and  $\mathbf{F} = \mathbf{F}_0 + \tilde{\mathbf{F}}$ , where  $\mathbf{F} = \{-F_0, 0, 0\}$  and the field  $\tilde{\mathbf{F}}$  is defined by the Poisson equation:

$$\text{div} \tilde{\mathbf{F}} = -\frac{4\pi eN}{\kappa_0} \delta[z] \int d\mathbf{p} \tilde{\Phi}, \quad (6)$$

where  $\kappa_0$  is the dielectric constant of the quantum well surroundings;  $\delta[z]$  is the Dirac function. The perturbations are assumed to be dependent on time  $t$  and  $x$  coordinate as follows:  $\tilde{\Phi}(\mathbf{p}, x, t) = \tilde{\phi}(\mathbf{p}) \exp[iqx - i\omega t]$ ,  $\tilde{\mathbf{F}}(x, z, t) = \tilde{\mathbf{f}}(z) \exp[iqx - i\omega t]$ . In this case the field induced by the perturbed electron gas has two components:  $\tilde{\mathbf{f}}(z) = \{\tilde{f}_x(z), 0, \tilde{f}_z(z)\}$ . The Fourier components  $\tilde{\phi}(\mathbf{p})$ ,  $\tilde{f}_x(z)$ ,  $\tilde{f}_z(z)$  are dependent on  $\omega$  and  $q$ .

The BTE in its general form of Eq. (5) can be simplified by adapting it to the problem under consideration as follows. Both contributions to the distribution function,  $\Phi_0$  and  $\tilde{\phi}$ , are approximated as sums of isotropic and anisotropic parts:<sup>15</sup>

$$\begin{aligned} \Phi_0(\mathbf{p}) &= \phi_0(p) + \phi_1(p) \delta(\theta), \\ \tilde{\phi}(\mathbf{p}) &= \tilde{\phi}_0(p) + \tilde{\phi}_1(p) \delta(\theta), \end{aligned} \quad (7)$$

where the two-dimensional vector  $\mathbf{p}$  is presented by its modulus  $p$  and the angle  $\theta$  to the  $X$ -axis.

The next simplifications are the following. In the passive region, for elastic momentum scattering it is easy to obtain  $\hat{L}_{el}\{\phi_0\} = \hat{L}_{el}\{\tilde{\phi}_0\} = 0$ . While in equations for anisotropic

parts,  $\phi_1, \tilde{\phi}_1$ , the elastic scattering integrals produce the relaxation terms  $-\{\phi_1, \tilde{\phi}_1\}/\tau_p$ . We suppose that the elastic scattering is due to interaction with acoustic phonons. Then, for two-dimensional electrons,  $\tau_p$  does not depend on the momentum/energy. In the active region, the collision operator describing optical phonon emission can be estimated as  $\hat{L}_{op}\Phi \sim \Phi/\tau_{op}^{em}$ , where the optical phonon emission time is the shortest time in the system ( $\tau_{op}^{em} \rightarrow 0$ ). Together with inequality (1), this provides the following conditions<sup>11</sup> for the isotropic parts of the distribution function:  $\phi_0(p \geq p_0), \tilde{\phi}_0(p \geq p_0) \approx 0$ . In contrast, the anisotropic parts of the distribution functions,  $\phi_1, \tilde{\phi}_1$ , are finite at  $p = p_0$  due to field induced electron stream in the momentum space. However, as discussed above, the number of streaming electrons in the active region is rapidly decreasing because of the optical phonon emission. As a result of these simplifications, the BTE is reduced to a system of coupled ordinary differential equations for  $\phi_0, \phi_1, \tilde{\phi}_0, \tilde{\phi}_1$  in the interval  $0 < p \leq p_0$ .

For the steady-state problem these equations are:

$$\begin{aligned} eF_0 \frac{d(p\phi_1)}{dp} &= 0 \\ eF_0 \left[ \pi \frac{d\phi_0}{dp} + \frac{1}{p} \frac{d(p\phi_1)}{dp} \right] &= -\frac{\phi_1}{\tau_p} \end{aligned} \quad (8)$$

Two first-order differential Eqs. (8) have to be supplied by two conditions to determine integration constants. One of these can be obtained from the normalization of the steady state function. We set  $\int \Phi_0(\mathbf{p})d\mathbf{p} = 1$ , then we have

$$\int_0^{p_0} p dp [2\pi\phi_0 + \phi_1] = 1. \quad (9)$$

The second condition follows from the above discussion:

$$\phi_0(p_0) = 0. \quad (10)$$

The spatial and temporal problem is described by equations:

$$\begin{aligned} i \left[ -\omega(2\pi\tilde{\phi}_0 + \tilde{\phi}_1) + \frac{qp}{m^*}\tilde{\phi}_1 \right] + e\frac{F_0}{p} \frac{d(p\tilde{\phi}_1)}{dp} &= 0 \\ i \left[ \left(-\omega - \frac{i}{\tau_p}\right)\tilde{\phi}_1 + \frac{qp}{m^*}(\pi\tilde{\phi}_0 + \tilde{\phi}_1) \right] + eF_0 \left[ \pi \frac{d\tilde{\phi}_0}{dp} \right. \\ \left. + \frac{1}{p} \frac{d(p\tilde{\phi}_1)}{dp} \right] &= e\tilde{f}_x \pi \frac{d\phi_0}{dp}, \end{aligned} \quad (11)$$

In order to obtain the "boundary" conditions for the latter system, we use the continuity equation, that follows from the BTE in its general form of Eq. (5):  $\int d\mathbf{p} \left[ \frac{\partial \Phi}{\partial t} + \frac{\mathbf{p}}{m^*} \frac{\partial \Phi}{\partial \mathbf{r}} \right] = 0$ .

Using our notation, it reads

$$\int_0^{p_0} p dp \left[ -\omega(2\pi\tilde{\phi}_0 + \tilde{\phi}_1) + q\frac{p}{m^*}\tilde{\phi}_1 \right] = 0. \quad (12)$$

Then with the use of the first equation from (11), we obtain:

$$p\tilde{\phi}_1|_{p \rightarrow 0} - p_0\tilde{\phi}_1(p_0) = 0. \quad (13)$$

The second boundary condition is similar to Eq. (10):

$$\tilde{\phi}_0(p_0) = 0. \quad (14)$$

The *ac*-electric field component,  $\tilde{f}_x$ , that enters into the right hand side of the second equation of the system (11), is defined via the Fourier component of the electrostatic potential,  $\tilde{\varphi}$ :  $\tilde{f}_x = -iq\tilde{\varphi}$ . The latter obeys the Poisson equation:

$$\frac{d^2\tilde{\varphi}}{dz^2} - q^2\tilde{\varphi} = \frac{4\pi eN}{\kappa_0} \delta(z) \int_0^{p_0} dp p [2\pi\tilde{\phi}_0 + \tilde{\phi}_1] \quad (15)$$

with the boundary conditions  $\tilde{\varphi}(z \rightarrow \pm\infty) = 0$ . These relations finalize the mathematical formulation of the steady-state and wave-like excitation problems for the streaming two-dimensional electron gas.

### III. SOLUTIONS OF EQUATIONS

To proceed further it is convenient to introduce the following dimensionless variables:

$$X = \frac{x}{l_F}, T = \frac{t}{\tau_F}, P = \frac{p}{p_0}, \Omega = \omega\tau_F, \Gamma = \frac{\tau_F}{\tau_p}, Q = ql_F. \quad (16)$$

We substitute  $p_0^2\phi_0 \rightarrow \phi_0$ ,  $p_0^2\tilde{\phi}_0 \rightarrow \tilde{\phi}_0$ , etc. Thus, the functions  $\phi_0$ ,  $\phi_1$ ,  $\tilde{\phi}_0$ ,  $\tilde{\phi}_1$  are now dimensionless.

#### A. Solutions for steady state problem

The solutions of Eqs. (8)-(10) for the steady state problem are

$$\phi_0(P) = \frac{-2\Gamma}{\pi[2+\Gamma]} \ln P, \quad (17)$$

$$\phi_1(P) = \frac{2}{[2+\Gamma]} \frac{1}{P} \quad (18)$$

Eqs. (17) describe the electron distribution quite well almost in the whole momentum space, except a narrow interval corresponding to the electron penetration into the active region given by Eq. (3) and the respective interval nearby  $p = 0$ .<sup>11</sup>

Having  $f_0$  and  $f_1$  one can calculate the average electron energy and the drift velocity:

$$\epsilon_{av} = \int d\mathbf{p} \frac{p^2}{2m^*} \Phi_0(\mathbf{p}) = \frac{8 + 3\Gamma}{12 [2 + \Gamma]} \hbar\omega, \quad (19)$$

$$v_{dr} = \int d\mathbf{p} \frac{p_x}{m^*} \Phi_0(\mathbf{p}) = \frac{1}{[2 + \Gamma]} \frac{p_0}{m^*}, \quad (20)$$

For the case of the strong inequality (2), we obtain the characteristics of the "ideal" electron streaming regime:  $\epsilon_{av} = \hbar\omega_0/3$ ,  $v_{dr} = p_0/2m^*$ .

## B. Solutions for the space and time dependent problem

Using the dimensionless variables of Eqs. (16) one can rewrite equations Eqs. (11) in the form:

$$\begin{aligned} i \left[ -\Omega \left( 2\pi P \tilde{\phi}_0 + P \tilde{\phi}_1 \right) + 2QP^2 \tilde{\phi}_1 \right] + \frac{d(P\tilde{\phi}_1)}{dP} &= 0, \\ i \left[ (-\Omega - i\Gamma) P \tilde{\phi}_1 + 2QP \left( \pi P \tilde{\phi}_0 + P \tilde{\phi}_1 \right) \right] & \\ + \left[ \pi \frac{d(P\tilde{\phi}_0)}{dP} - \pi \tilde{\phi}_0 + \frac{d(P\tilde{\phi}_1)}{dP} \right] &= \pi \frac{\tilde{f}_x}{F_0} P \frac{d\phi_0}{dP}. \end{aligned} \quad (21)$$

The following substitutions

$$\begin{aligned} \pi P \tilde{\phi}_0 &= \chi_0 \exp [i (\Omega P - QP^2)], \\ P \tilde{\phi}_1 &= \chi_1 \exp [i (\Omega P - QP^2)], \end{aligned} \quad (22)$$

transform Eqs (21) to the simpler form

$$\begin{aligned} \frac{d\chi_1}{dP} &= 2i\Omega\chi_0, \\ \frac{d\chi_0}{dP} + \left[ 3i\Omega - \frac{1}{P} \right] \chi_0 + \Gamma\chi_1 &= \pi \frac{\tilde{f}_x}{F_0} P \frac{d\phi_0}{dP} \\ &\times \exp [-i (\Omega P - QP^2)]. \end{aligned} \quad (23)$$

The latter system of two equations can be reduced to a single equation for the function,  $\chi_1(P)$ , that we present as

$$\frac{d^2\chi_1}{dP^2} + \left[ b - \frac{1}{P} \right] \frac{d\chi_1}{dP} + c\chi_1 = \frac{\tilde{f}_x}{F_0} R(P | \Omega, Q), \quad (24)$$

where we designate

$$\begin{aligned} b &= 3i\Omega, \quad c = 2i\Omega\Gamma, \\ R(P | \Omega, Q) &= 2\pi i\Omega P \frac{d\phi_0}{dP} \exp [-i (\Omega P - QP^2)]. \end{aligned} \quad (25)$$



Note that, in the left hand side of Eq. (24), the parameters,  $b$ ,  $c$ , are dependent only on  $\Omega$ , while the right hand side parametrically depends on both  $\Omega$  and  $Q$ . From Eqs. (13), (14) and the first equation of the system (23) it follows the boundary conditions to Eq. (24):

$$\begin{aligned}\chi_1(0) &= \chi_1(1) \exp [i (\Omega - Q)] , \\ \frac{d\chi_1}{dP}(1) &= 0 .\end{aligned}\tag{26}$$

The general solution to Eq. (24) can be presented as

$$\begin{aligned}\chi_1(P) &= C_1\Psi_1(P) + C_2\Psi_2(P) + \\ \frac{\tilde{f}_x}{F_0} &\left[ \Psi_1(P) \int_P^1 \frac{R(P')\Psi_2(P')}{W_\Omega(P')} dP' - \Psi_2(P) \int_P^1 \frac{R(P')\Psi_1(P')}{W_\Omega(P')} dP' \right]\end{aligned}\tag{27}$$

where  $\Psi_1(P)$ ,  $\Psi_2(P)$  are two independent solutions of the congruent homogeneous equation,  $W_\Omega(P)$  is the Wronskian of this equation,  $C_1$ ,  $C_2$  are arbitrary constants. The functions  $\Psi_1(P)$  and  $\Psi_2(P)$  can be expressed via the Kummer functions of first and second kinds,<sup>18</sup>  $M(u, w, z)$  and  $U(u, w, z)$ , respectively:

$$\begin{aligned}\Psi_1(P) &= P^2 \exp(-\alpha P)M[\beta, 3, \epsilon P] , \\ \Psi_2(P) &= P^2 \exp(-\alpha P)U[\beta, 3, \epsilon P] ,\end{aligned}$$

with  $\epsilon = \sqrt{b^2 - 4c}$ ,  $\alpha = (b + \epsilon)/2$  and  $\beta = 3/2 - \tilde{b}/2\epsilon$ .

For the problem under consideration, the constants  $C_1$  and  $C_2$  should be found by using the boundary conditions (26). The latter result in the following equations:

$$C_1 \frac{d\Psi_1}{dP}(1) + C_2 \frac{d\Psi_2}{dP}(1) = 0 \tag{28}$$

$$\begin{aligned}C_1 \{ \Psi_1(0) - \Psi_1(1) \exp [i (\Omega - Q)] \} + C_2 \{ \Psi_2(0) - \Psi_2(1) \exp [i (\Omega - Q)] \} = \\ - \frac{\tilde{f}_x}{F_0} [ \Psi_1(0)J_2(0) - \Psi_2(0)J_1(0) ] ,\end{aligned}\tag{29}$$

where  $J_{1,2}(P) \equiv \int_P^1 \frac{R(P')\Psi_{1,2}(P')}{W_\Omega(P')} dP'$ . The  $ac$  electric field,  $\tilde{f}_x$ , that appears in the right hand side of Eq. (29), is defined by the Poisson Eq. (15):

$$\begin{aligned}\frac{\tilde{f}_x}{F_0} &= \text{sgn}(Q) \frac{2\pi ieN}{\kappa_0 F_0} \int_0^1 dP P \left[ 2\pi \tilde{\phi}_0 + \tilde{\phi}_1 \right] = \\ \text{sgn}(Q) \frac{2\pi ieN}{\kappa_0 F_0} &\int_0^1 dP \left[ \chi_1 - \frac{i}{\Omega} \frac{d\chi_1}{dP} \right] \exp [i (\Omega P - Q P^2)] ,\end{aligned}\tag{30}$$

where  $\text{sgn}(Q)$  stands for sign of  $Q$ . Substituting (27) to Eq. (30) one can find  $\tilde{f}_x$  as a linear homogeneous form of the constants  $C_1, C_2$ :

$$\frac{\tilde{f}_x}{F_0} = \mathcal{N} (A_1 C_1 + A_2 C_2) , \tag{31}$$

where  $A_{1,2} = A_{1,2}\{\Psi_1, \Psi_2|\Omega, Q\}$  are expressed via bulky integrals from some combinations of the functions  $\Psi_1$  and  $\Psi_2$ . We introduce the parameter

$$\mathcal{N} = \frac{N}{N_{ch}}, \quad N_{ch} \equiv \frac{\kappa_0 F_0}{2\pi e}, \quad (32)$$

which has the meaning of a dimensionless electron concentration. From the structure of Eq. (29) it follows that this parameter determines the coupling of the dynamics of individual electrons and their collective motion arising due to the self-consistent electric field,  $\tilde{\mathbf{f}}$ . Eqs. (28), (29) supplemented by the relationship (31) compose the system of homogeneous linear algebraic equations for the constants  $C_1, C_2$ . The solvability condition of this system is determined by the zero of the associated determinant,  $\Delta(\Omega, Q) = 0$ . The latter condition gives the dispersion relation,  $\Omega(Q)$ , for required excitations of the drifted electron gas.

### C. Frequency and wavevector dispersion of electron conductivity and dielectric permittivity of the electrons.

The solvability of the obtained equations can be also presented in a more usual form. Indeed, the high frequency current can be calculated as

$$\tilde{j}_x = -\frac{eNp_0}{m^*} \int_0^1 dP P^2 \tilde{\phi}_1(P), \quad (33)$$

where parametrically dependent on  $\Omega$  and  $Q$  function  $\tilde{\phi}_1(P)$  is the solution of Eqs. (22), (27), (28), (30) obtained at a given  $\tilde{f}_x/F_0$ . Then, the high frequency conductivity is

$$\begin{aligned} \sigma(\Omega, Q) &= \frac{\tilde{j}_x}{\tilde{f}_x} = \frac{eNp_0}{mF_0} \nu(\Omega, Q) \equiv e\mu_0 N \frac{F_{cr}}{F_0} \nu(\Omega, Q), \\ \nu(\Omega, Q) &\equiv -\frac{F_0}{\tilde{f}_x} \int_0^1 dP P^2 \tilde{\phi}_1(P), \end{aligned} \quad (34)$$

where  $\mu_0 = e\tau_p/m$  is the low field mobility,  $\nu(\Omega, Q)$  does not depend on  $\tilde{f}_x/F_0$  and has a meaning of dimensionless electron mobility dependent on both the frequency and the wavevector.

With the help of Eq. (34), one can calculate the dielectric permittivity of the electrons:

$$\epsilon(\Omega, Q) = 1 + i2\mathcal{N} \frac{|Q|}{\Omega} \nu(\Omega, Q). \quad (35)$$

It can be easily proved that the usual requirement

$$\epsilon(\Omega, Q) = 0, \quad (36)$$

that defines the possible *collective* excitation modes of the electron gas, is identical to the above obtained solvability condition.

For what follows, it is useful to discuss briefly some properties of the high frequency mobility,  $\nu(\Omega, q)$ . Fig. 1 shows the results of calculations of  $\nu(\Omega, Q)$  for  $F_0/F_{cr} = 3$ . The OPTTR becomes apparent near  $\Omega = \pm 2\pi$ . Indeed, one can see typical frequency dispersion of the conductivity in narrow frequency intervals and, particularly, a change of the sign of the dynamic conductivity ( $Re[\nu] < 0$ ). The latter feature has been in focus of previous studies.<sup>6,8,9,11</sup> At  $Q \neq 0$ , drift of the electrons is revealed: the characteristic feature arises at  $\Omega \approx V_{dr}Q$ , where  $V_{dr}$  is the dimensionless drift velocity defined as  $V_{dr} = 2v_{dr}m/p_0$  with the field dependent  $v_{dr}$  given by Eq. (20). Besides, a negative dynamic conductivity occurs at the Cerenkov region,  $0 < \Omega < V_{dr}Q$ , while the OPTTR frequencies are shifted by factor  $V_{dr}Q$ . Note, the absolute values of  $\nu(\Omega, Q)$  are relatively small. This is typical for conditions of the streaming regime, when the drift velocity saturates and the differential mobility tends to zero.

#### IV. SOLUTIONS AT $\mathcal{N} \rightarrow 0$ .

First, we study the space and time dependent solutions neglecting self-consistent electric field  $\tilde{\mathbf{f}}$ . According to the relationship (31), this corresponds to the limiting case

$$\mathcal{N} \ll 1. \quad (37)$$

In this limit, the electron gas excitations can be thought as *phased* motion of the electrons in the real space and the momentum space under the conditions of cyclic dynamics of individual electrons. Importantly, all results for this limit depend on the single parameter,  $F_0/F_{cr} = \tau_p/\tau_F = 1/\Gamma$ .

For such a case, from Eqs. (28) and (29) we immediately obtain the condition of solvability of these equations in the form

$$\Delta_0(\Omega, Q) = \Psi_1(0)\frac{d\Psi_2}{d\rho}(1) - \Psi_2(0)\frac{d\Psi_1}{d\rho}(1) - W_\Omega(1)\exp[i(\Omega - Q)] = 0, \quad (38)$$

that can be rewritten as

$$\exp(-iQ) = \frac{\Psi_1(0)\frac{d\Psi_2}{d\rho}(1) - \Psi_2(0)\frac{d\Psi_1}{d\rho}(1)}{W_\Omega(1)} \exp(-i\Omega) \equiv \mathcal{S}(\Omega', \Omega''|F_0). \quad (39)$$

In the latter form, the left hand side depends on  $Q$ , while the right hand side is a function of  $\Omega$ . We will look for wave-like excitations with a real wavevector,  $Q$ , while the frequency can be a complex value,  $\Omega = \Omega' + i\Omega''$ . To find  $\Omega'$  and  $\Omega''$  at a given  $Q$  we have two equations

$$abs[\mathcal{S}(\Omega', \Omega'')] = 1, \quad (40)$$

$$Q = -arg[\mathcal{S}(\Omega', \Omega'')] \pm 2\pi k, \quad (41)$$

where  $k$  is an integer,  $k = 0, 1, 2, \dots$ . Here we introduce the absolute value,  $abs[\mathcal{S}]$ , and the phase,  $arg[\mathcal{S}]$ , of the complex function  $\mathcal{S}(\Omega', \Omega'')$ . Eq. (40) defines the damping of the excitations,  $\Omega''$ , as a function of the frequency  $\Omega'$ . Then, Eq. (41) defines implicitly the dispersion relation of sought-for wave excitations,  $\Omega'(Q)$  for the limiting case of Eq. (37).

To understand the nature of the solutions of Eq. (40), one should analyze the following function of two variables  $\mathcal{G}(\Omega', \Omega'') = abs[\mathcal{S}(\Omega', \Omega'')] - 1$ . This function parametrically depends on a single value: the dimensionless field  $F_0/F_{cr}$ . In Fig. 2, a typical density plot of  $\mathcal{G}(\Omega', \Omega'')$  is presented for  $F_0/F_{cr} = 3$  (see below discussion of actual parameters for particular materials). As seen from this figure, there are two kinds of solutions,  $\Omega'' = \Omega''[\Omega']$ . The first is characterized by small  $\Omega''$  and, particularly,  $\Omega''(\Omega' = 0) = 0$ . The second kind of solutions gives  $\Omega''$  of the order of  $\Omega'$ . Below we will concentrate on the first kind of solutions, because the electron gas excitations corresponding to such solutions are weakly damped.

From Eq. (41), it follows that there is an infinite set of branches of the dispersion relation corresponding to different values of the integer  $k$ . We will call the branch of  $k = 0$  as the acoustic-like dispersion branch. From Eqs. (40) and (41), for the acoustic branch one can find a function  $\Omega = \Omega^0(Q)$ . Then, any other 'satellite' branch can be obtained by a simple translation in the  $\{\Omega, Q\}$ -plane along the  $Q$ -axe:  $\Omega = \Omega^k(Q) = \Omega^0(Q \pm 2\pi k)$ . The "basic vector" of translation is  $Q_0 = 2\pi$ . Its dimension value is  $2\pi/l_F$ . In the real space, this value corresponds to a wavelength of the excitation strictly equal to the characteristic spatial period of the cyclic electron motion,  $l_F$ . For the acoustic branch, we find that  $\Omega^0 \approx V_{dr}Q$  at  $Q \rightarrow 0$ . At finite  $Q$ , the acoustic branch can be obtained numerically: the result is shown in Fig. 3 (a). In this figure, we presented also two satellite branches with  $k = -1, 1$ . The latter branches have finite frequencies at  $Q \rightarrow 0$ , i.e., they can be thought as of optical type. Interestingly, the frequencies of the satellite branches at finite wavevectors  $Q = Q_0 k$  are *exactly* zero. This means that the corresponding electron gas excitations are *standing* waves. For convenience in Fig. 3 (b), we show also the imaginary part of the frequency,  $\Omega''(Q)$ , for

each of the branches. The absolute values of  $\Omega''$  are small in comparison with  $\Omega'$ .<sup>19</sup> The solutions corresponding to the standing waves have zero damping,  $\Omega''(kQ_0) = 0$ .

For the latter particular case ( $\Omega = 0$ , while  $\Gamma \neq 0$ ), the solutions can be found in an explicit form. Indeed, from Eqs. (23) we find  $\chi_1 = C = \text{constant}$ ,  $\chi_0 = -C\Gamma P \ln P$ . Then, from the boundary conditions (26) we find the allowed  $Q = 2\pi k$ ,  $k \neq 0$ . According to Eqs (22), contributions to the distribution function are

$$\tilde{\phi}_0 = -\frac{C\Gamma}{\pi} \ln P \times \exp(-i2\pi k P^2), \quad (42)$$

$$\tilde{\phi}_1 = \frac{C}{P} \times \exp(-i2\pi k P^2), \quad (43)$$

Interestingly, the Fourier component of the perturbed electron density corresponding to these solutions is not zero, while the perturbation of the average electron velocity is zero, i.e. there are no electron fluxes in real space.

Additional analytical results can be obtained for the ultimately simple case adequate to  $\Gamma = 0$  (absence of any scattering in the passive region). In this limit, from Eqs. (23), we obtain  $\chi_0 = 0$ ,  $\chi_1 = C = \text{constant}$ . The corresponding contributions to the distribution function are:

$$\tilde{\phi}_0 = 0, \quad \tilde{\phi}_1 = \frac{C}{P} \exp[i(\Omega P - Q P^2)].$$

Then, from the boundary conditions (26) we find  $\exp[i(\Omega - Q)] = 1$ , i.e., the dispersion relation gives an infinite set of straight lines:  $\Omega_{\Gamma=0}^k(Q) = Q + 2\pi k$ ,  $k = 0, \pm 1, \dots$  ( $\Gamma = 0$ ). At nonzero but small  $\Gamma$ , this dispersion relation can be corrected by using the perturbation method:  $\Omega = \Omega_{\Gamma=0}^k + \Gamma \mathcal{B}(Q + 2\pi k)$ , where the function  $\mathcal{B}(X)$  is defined as

$$\mathcal{B}(X) = 2X \int_0^1 dx x e^{-i3Xx} \int_1^x \frac{dy}{y} e^{i3Xy}.$$

Near the points  $Q = -2\pi k$ , where  $\Omega_{\Gamma=0}^k$  is small, we obtain approximately

$$\Omega \approx (Q + 2\pi k) \left(1 - \frac{\Gamma}{2}\right) - i\frac{\Gamma}{3}(Q + 2\pi k)^2.$$

Thus, electron momentum dissipation in the passive region leads to the damping of the wave excitations, as well as to renormalization of the excitation frequency. However, the standing waves are not damped.

The found dispersion relation and solutions can be explained by time-dependent *phased* motion of many electrons in both the real space and the momentum space. The properties

of such a phased motion are very distinct for different  $Q$  and  $k$ . Indeed, for the acoustic branch at  $\Omega$ ,  $Q \rightarrow 0$  the solutions correspond to the simple drift of a perturbed electron concentration with velocity  $V_{dr}$  (this type of solutions can be obtained, particularly, in the simplest hydrodynamical models). At  $k \neq 0$  and small  $Q$  (optical-like branches), the time-dependent phased motion occurs mainly in the momentum space. At  $k \neq 0$ ,  $Q \approx kQ_0$ , the electron motion in the real space is phased with that in the momentum space, but it is time independent.

## V. SOLUTIONS AT $\mathcal{N}$ OF A FINITE VALUE.

For the case of a finite value of  $\mathcal{N}$ , when collective charge effects are involved, we performed a numerical analysis of the equations. Before presenting this analysis, we note that, due to the scaling given by Eqs. (16), the results obtained for  $\mathcal{N} = 0$  were dependent only on the dimensionless parameter  $F_0/F_{cr}$ . Now, for a given  $\mathcal{N}$  we calculate  $\nu(\Omega, Q)$  and  $\epsilon(\Omega, Q)$  according to Eqs. (34), (35), then we solve Eq. (36) for the complex frequency  $\Omega$  at a given real wavevector  $Q$ . Representative examples of these calculations are given in Fig. 4, where the real and imaginary parts of  $\Omega$  are shown as functions of  $Q$  for three branches of excitation spectra at  $F_0/F_{cr} = 3$  and  $\mathcal{N} = 7.4$ . Comparison of the results for the real part of the frequency,  $\Omega'$ , with those presented in Fig. 3 shows that, at a finite  $\mathcal{N}$ , noticeable changes occur for the acoustic branch of the excitation spectra, while changes of the optical-like branches ( $k = \pm 1$ ) are much smaller. Particularly, there is no effect of  $\mathcal{N}$  on the existence of the standing waves ( $\Omega = 0$ ), which have the same spatial periods ( $Q = 2\pi k$ ). A more detailed evolution of the acoustic-like branch when  $\mathcal{N}$  varies is illustrated in Fig. 5 (a). Comparing the damping of the excitations,  $\Omega''$ , presented in Fig. 4 (b) one can make similar conclusion: at finite values of  $\mathcal{N}$  the damping of the acoustic-like excitation branch increases significantly, while that of the optical-like branches is less affected. Specifically, the standing waves remain strictly undamped. In Fig. 5 (b) the damping of the acoustic-like branch is presented for different  $\mathcal{N}$ .

Remarkably, the solutions for the standing waves can be obtained *exactly* for arbitrary  $\mathcal{N}$ . The solutions include, particularly, the expression for the amplitude of the electric field,  $\tilde{f}_x$ , associated with space and time dependent redistribution of the charged carriers. These

solutions are:

$$\begin{aligned} \Omega = 0, Q = 2\pi k, \\ \tilde{\phi}_0 = -\frac{C\Gamma}{\pi} \frac{2 + \Gamma + 2i\Gamma\mathcal{N}I_1(k)}{2 + \Gamma + 4i\Gamma\mathcal{N}I_2(k)} \ln P \times \exp(-i2\pi k P^2), \\ \tilde{\phi}_1 = \frac{C}{P} \times \exp(-i2\pi k P^2), \\ \frac{\tilde{f}_x}{F_0} = i\mathcal{N}C \frac{[2 + \Gamma][I_1(k) - 2\Gamma I_2(k)]}{2 + \Gamma + 4i\Gamma\mathcal{N}I_2(k)}, \end{aligned} \quad (44)$$

(45)

Here  $C$  is an arbitrary constant, functions  $I_1(k)$  and  $I_2(k)$  are

$$I_1(k) = \int_0^1 dP e^{-i2\pi k P^2}, \quad I_2(k) = \int_0^1 dP P \ln P e^{-i2\pi k P^2}.$$

As indicated above, the found solutions correspond to a time-dependent motion of the electrons in real space highly correlated with that in momentum space. Spatial charge effects are related to electron behavior in real space. To analyze them, one can introduce the concentration of the "isotropic" electrons,  $\tilde{N}_0$ , and the concentration of the "streaming" electrons,  $\tilde{N}_1$ , which are determined through the disturbed distributions  $\tilde{\phi}_0$  and  $\tilde{\phi}_1$ , respectively. The total perturbed concentration of the excitation wave is  $\tilde{N} = \tilde{N}_0 + \tilde{N}_1$ . To understand the main characteristics of the time and real space dependences of these concentrations we neglect the small damping of the excitations, so that the dependences are

$$\begin{aligned} \tilde{N}_0(X, T) &= \tilde{N}_0(Q, k) \cos[\Omega^k(Q)T - QX + \delta_0], \\ \tilde{N}_1(X, T) &= \tilde{N}_1(Q, k) \cos[\Omega^k(Q)T - QX + \delta_1]. \end{aligned} \quad (46)$$

Here we take into account that a given spectrum branch number,  $k$ , and wavevector,  $Q$ , determine the excitation frequency,  $\Omega^k(Q)$ , and the particular solutions. Then,  $\delta_0$  and  $\delta_1$  are phase shifts dependent on  $Q$  and  $k$ .

In Fig. 6 the relative amplitudes of concentrations of "isotropic", and "anisotropic" electrons, and their phase difference  $\delta(Q, k) \equiv \delta_0(Q, k) - \delta_1(Q, k)$  are shown for three excitation branches presented in Fig. 4. The results illustrate useful symmetry properties of these functions. Indeed, for the acoustic branch ( $k = 0$ ), the relative amplitudes,  $\tilde{N}_{0,1}(Q, k)/\tilde{N}(Q, k)$ , are even functions of  $Q$ , while the phase difference is an odd function of  $Q$ . For a given optical branch, the relative amplitude is a strongly asymmetrical function of  $Q$ . However, there are simple relationships between the characteristics of two branches with  $\pm k$ . At given

$k$  and  $Q$ , the relative amplitudes coincides with those of the branch  $-k$  at the wavevector  $-Q$ , while  $\delta(Q, k) = -\delta(-Q, -k)$ . Significantly the different character of the excitations corresponding to the acoustic and optical branches can be seen from Fig. 6 for small wavevectors. Indeed, for the acoustic branch all functions,  $\tilde{N}_0(Q, 0)$ ,  $\tilde{N}_1(Q, 0)$  and  $\tilde{N}(Q, 0)$  are of the same order of magnitude while the phase shift  $\delta \neq \pm\pi$ . For the optical branches, we obtain  $\tilde{N}_0(Q, k) \approx \tilde{N}_1(Q, k) \gg \tilde{N}(Q, k)$  and  $\delta \approx \pi$ , i.e., the concentrations of the isotropic and streaming electrons oscillate in antiphase,  $\tilde{N}$  and the space charge are almost zero. For finite  $Q$ , the excitations are always accompanied by a space charge wave. At  $k = 1$  (-1) and  $-2\pi < Q < 0$  ( $0 < Q < 2\pi$ ), the phase velocity of the excitation is negative and all disturbed electrons concentrations are of the same order of magnitude. Otherwise, the phase velocity of the excitation is positive. For the developed streaming effect ( $F_0 \gg F_{cr}$ ),  $\tilde{N}_1$  dominates over  $\tilde{N}_0$ .

Thus, the accounting of space charge effects does not change considerably the basic properties of the electron excitations under streaming transport regime. The multi-branch character of the excitation spectra, the occurrence of the standing waves and other properties can be observed at finite electron concentrations. The space charge accompanying the wave excitations affects mainly their damping. Space charge induced increase of damping of electron excitations is characteristic for regimes of electron motion with considerable dissipation.<sup>20</sup>

## VI. DISCUSSION AND SUMMARY

The cyclic electron motion caused by strongly inelastic processes (optical phonon emission) is characteristic for many polar materials and associated heterostructures subjected to high electric field at low temperatures. The characteristic time period,  $\tau_F$ , and spatial period,  $l_F$ , of this motion depend on the applied field,  $F$ . In steady state regime, such a motion reveals itself via the formation of a sufficiently anisotropic distribution function and quasi-saturation of the drift velocity, the average energy, etc. In time (frequency) domain, the cyclic electron motion gives rise to the specific optical phonon transient time resonance at frequencies defined by the time-of-flight,  $\omega \approx 2\pi/\tau_F$ . In real space, this kind of motion causes a spatial modulation of the electron concentration and velocity with the period  $l_F$ , which has been observed in structures of finite size. It is believed that the cyclic electron



dynamics should be more pronounced in low-dimensional structures.

Using the BTE, we have developed an approximate approach that permits us to analyze *coupled spatio-temporal dynamics* of two-dimensional electron gas under conditions of the cyclic motion. As a results, we have found a novel type of excitations of the drifting electron gas. These wave-like excitations are periodic in time and weakly damped oscillations of the electrons in both real and momentum spaces. Their frequency-wavevector relations consist of an infinite number of continuous branches  $\omega^k(q)$ ,  $k = 0, \pm 1, \pm 2, \dots$

The specific character of the correlated motion of electrons in the wave excitations strongly depends on the branch number  $k$  and the wavevector  $q$ . Thus, for  $k = 0, q \rightarrow 0$ , we have obtained  $\omega^0 \propto q$ , the electron motion is phased, mainly, in the real space, the excitation is conveyed by a space charge wave. This excitation can be defined as of acoustic type. For  $k \neq 0$  and  $q \rightarrow 0$ , the excitations represent, mainly, strong oscillations in the momentum space (time-dependent redistribution between 'isotropic' and 'streaming' groups of the electrons). While the space charge is practically absent. These excitations can be defined as of optical type. Each of the  $\omega^k(q)$ -branches once crosses the line  $\omega = 0$  at  $q = 2\pi k/l_F$ . This implies the existence of standing waves with wavelength,  $\lambda$ , related to the spatial period of the cyclic motion as  $\lambda = l_F/k$ . For the standing waves, electron motion in real and momentum spaces is phased, but time independent. The found excitations are weakly damped. Their damping is caused by quasi-elastic scattering of electrons and formation of a space charge. The standing waves are undamped.

Now we shall discuss the cyclic electron motion and the existence of the wave-like excitations in real polar heterostructures with two-dimensional electrons. For polar materials, the typical optical phonon energy is 30...100 *meV*. Due to the exponential temperature dependence of the optical phonon absorption time ( $\propto e^{-\hbar\omega_0/k_B T}$ ), this process is negligible at low temperatures. For two examples given below, the absorption time is more than  $10^4$  times larger than the emission time at  $T \leq 100 K$ . Other necessary and sufficient conditions for the realization of these effects are presented by Eqs. (1) and (2). These conditions contain two material parameters, the elastic scattering time in the passive region,  $\tau_p$ , and the optical phonon emission time,  $\tau_{op}^{em}$ . At low temperatures, the former time can be estimated by the use of data on the low-field mobility,  $\mu_0$ . The latter time can be found, for example, exploiting the dielectric continuum model of the optical phonons and the Frohlich electron-phonon interaction.<sup>21,22</sup> To avoid effects of electron-electron collisions on the cyclic motion,

the electron concentration should be less than  $10^{12} \text{ cm}^{-2}$ .<sup>12</sup>

First, we consider AlGaIn/GaN heterostructures. For two-dimensional electrons in GaN-channels, the optical phonon emission is estimated to be  $\tau_{op}^{em} \approx 0.01..0.02 \text{ ps}$ .<sup>11,13</sup> The highest low-field mobility was measured at sub-Helium temperatures for structures with low density of dislocations:  $\mu_0 = (1..2) \times 10^5 \text{ cm}^2/\text{Vs}$ .<sup>23-25</sup> These results were obtained for sufficiently low electron concentrations:  $N \approx (4..10) \times 10^{11} \text{ cm}^{-2}$ . The measurements evidence that in such structures at moderately low temperature the mobility is limited by acoustic phonon scattering. At  $T = 50..100 \text{ K}$ , the acoustic phonon limited mobility is  $\approx (5..2.5) \times 10^4 \text{ cm}^2/\text{Vs}$ .<sup>24-26</sup> For numerical estimations, we choose a modest value of the mobility,  $\mu_0 = 10^4 \text{ cm}^2/\text{Vs}$ , then we find  $\tau_p \approx 1 \text{ ps}$ . Thus the strong inequality (1) is met. For further calculations we use the following parameters:  $m^* = 0.2m_0$  ( $m_0$  is the free electron mass),  $\hbar\omega_0 = 92 \text{ meV}$ ,  $\kappa_0 = 9$ . Then, according to Eq. (4), the electric field for the onset of the studied effects is  $F_{cr} \approx 4.7 \text{ kV/cm}$ . Thus, the numerical results shown in Figs. 4 and 5 correspond to an applied field  $F \approx 13.7 \text{ kV/cm}$ . The temporal and spatial periods of the cyclic motion are  $\tau_F \approx 0.33 \times 10^{-12} \text{ s}$  and  $l_F \approx 6.6 \times 10^{-6} \text{ cm}$ , respectively. According to Eq. (37), the characteristic electron concentration, for which the parameter  $\mathcal{N} = 1$ , is estimated to be  $N_{ch} = 1.4 \times 10^{11} \text{ cm}^{-2}$ . Having the scaling parameters  $\tau_F$ ,  $l_f$ ,  $N_{ch}$  and using the results of Figs. 4, 5 one can recover the dimensional characteristics of the wave excitations. For example, the frequency of the lowest optical-like branches at  $q \rightarrow 0$  is found to be  $\omega^{\pm 1}(q \rightarrow 0) = 1.5 \times 10^{13} \text{ s}^{-1}$ , its damping equals  $\gamma = 6 \times 10^{11} \text{ s}^{-1}$ . Undamped standing waves are realized for a wavevector equal to  $q = \pm 9.4 \times 10^5 \text{ cm}^{-1}$ . For the same  $q$ , the frequency (the damping) of the acoustic and optical branches are  $\omega \approx 2 \times 10^{13} \text{ s}^{-1}$  ( $\gamma \approx 1.2 \times 10^{12} \text{ s}^{-1}$ ) and  $\omega \approx 3.6 \times 10^{13} \text{ s}^{-1}$  ( $\gamma \approx 6 \times 10^{11} \text{ s}^{-1}$ ), respectively.

As second example of two-dimensional systems, where the discussed effects can be observed, we consider ZnO/MgZnO heterostructures. For these strongly polar oxide heterostructures, low field mobilities as high as  $4 \times 10^5 \text{ cm}^2/\text{Vs}$  were measured<sup>27</sup> at sub-Helium temperature and electron concentrations  $(1..4) \times 10^{11} \text{ cm}^{-2}$ . Above Helium temperature, it was found a phonon limited mobility temperature dependence:  $\mu_0 \propto T^{-3/2}$ . Particularly, for  $T \approx 10 \text{ K}$ , it is achieved  $\mu_0 \approx (2..4) \times 10^4 \text{ cm}^2/\text{Vs}$ .<sup>27,28</sup> For numerical estimates, we set  $\mu_0 = 10^4 \text{ cm}^2/\text{Vs}$ ,  $m^* = 0.3m_0$ ,  $\hbar\omega_0 = 72 \text{ meV}$ ,  $\kappa_0 = 8.1$ ,  $\kappa_\infty = 3.7$ . Then, we obtain  $\tau_{op}^{em} = 0.005..0.01 \text{ ps}$ ,  $\tau_p \approx 2 \text{ ps}$ , i.e., the necessary condition of Eq. (1) holds. The critical field is  $F_{cr} = 2.9 \text{ kV/cm}$ . For these parameters of the ZnO/MgZnO heterostructure, results

presented in Figs. 4 and 5 correspond to the applied field  $F \approx 9.7 \text{ kV/cm}$ . The periods of the relevant cyclic motion are  $\tau_F \approx 0.6 \times 10^{-12} \text{ s}$  and  $l_F \approx 0.8 \times 10^{-5} \text{ cm}$ . The characteristic electron concentration  $N_{ch}$  equals  $\approx 0.7 \times 10^{11} \text{ cm}^{-2}$ . With these scaling parameters and the results of Figs. 4, 5 one can recover the dimensionless characteristics of the wave excitations.

Summarizing, we have analyzed the low-temperature behavior of nonequilibrium two-dimensional electron gas in polar heterostructures subjected to moderately high electric fields. At low temperatures, when the optical phonon emission is the fastest relaxation process and an almost cyclic motion of individual electrons occurs, we have found the existence of collective wave-like excitations of the electrons. These wave-like excitations are periodic in time and weakly damped oscillations of the electrons in both real and momentum spaces. The excitation spectra are of multi-branch character, each of the spectra branches showing considerable spatial dispersion. There are one acoustic-type and a number of optical-type excitation spectra branches. Their small damping is caused by quasi-elastic scattering of electrons and formation of a relevant space charge. There are also waves with zero frequency and finite spatial periods - the standing waves. The studied excitations of the electron gas can be also interpreted as synchronous in time and real space manifestation of the optical phonon transit time resonance. Remarkably, these wave-like excitations exist in the electron gas even in the presence of significant dissipation through optical phonon emission. Estimations of the parameters of the excitations for two examples of polar two-dimensional heterostructures, GaN/AlGa<sub>N</sub> and ZnO/MgZnO, have shown that the excitation frequencies and the standing wave periods are in THz-frequency range and sub-micrometer region, respectively.

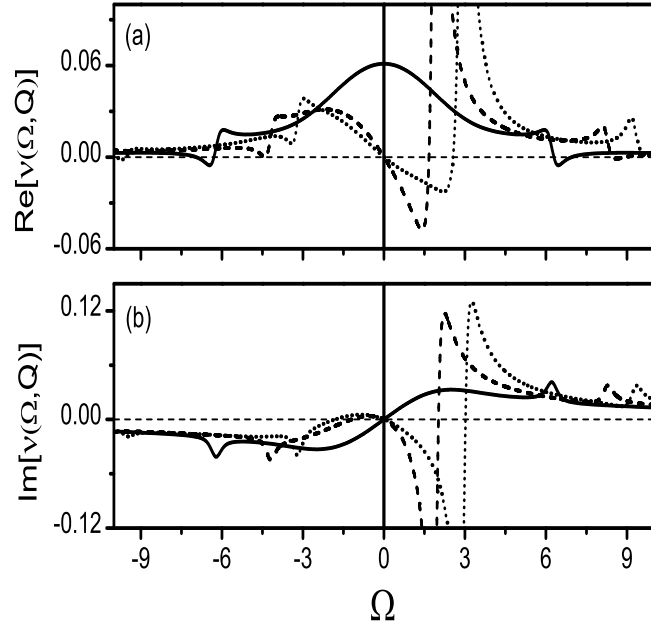


FIG. 1: Real (a) and imaginary (b) parts of the dimensionless high frequency mobility of Eq. (34) as functions of  $\Omega$  for different  $Q$ . Results are presented for  $F_0/F_{cr} = 3$ . Full, dashed and dotted lines correspond to  $Q = 0, 1, 2$ , respectively.

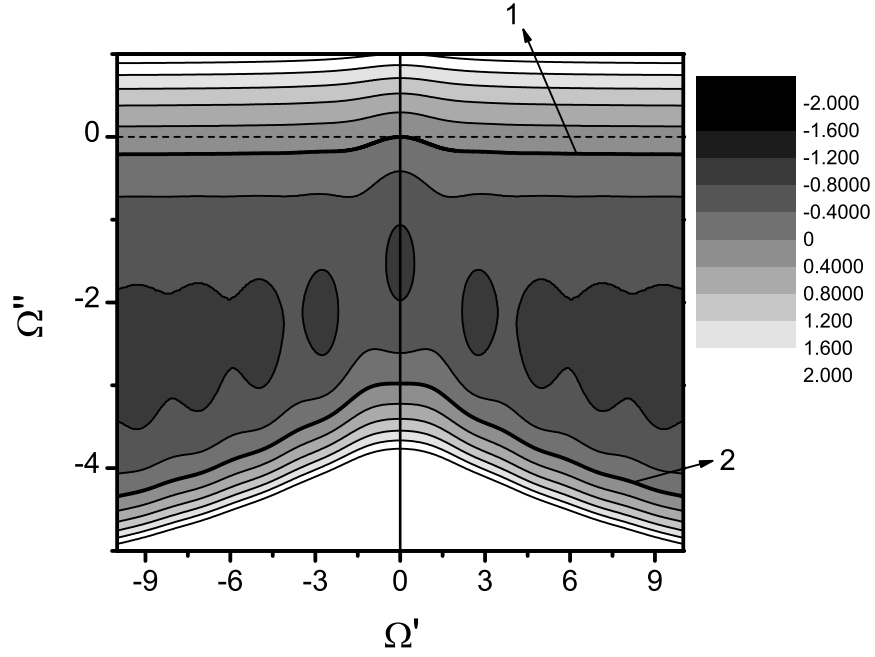


FIG. 2: Density plot of the function  $\mathcal{G}(\Omega', \Omega'')$ . Curves 1 and 2 correspond to  $\mathcal{G} = 0$  and present  $\Omega''(\Omega')$ -dependencies, i.e., the damping of the excitations.

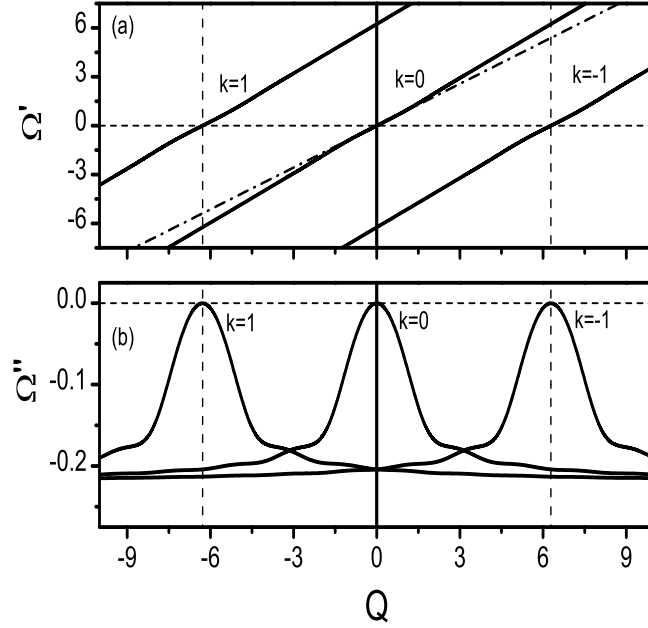


FIG. 3: Real (a) and imaginary (b) parts of the frequency as functions of the wavevector found from Eqs. (40), (41) for three branches of the dispersion relation at  $F_0/F_{cr} = 3$ . Dash-dotted line corresponds to  $\Omega' = V_{dr}Q$ . The vertical dashed lines mark wavevectors equal to  $Q = \pm 2\pi$ . Note that the vertical scales in (a) and (b) are very different.

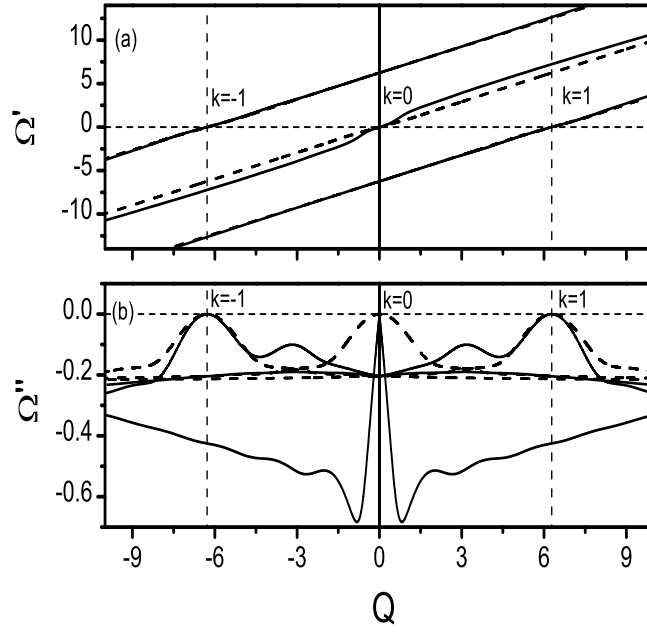


FIG. 4: The same as in Fig. (3) at  $\mathcal{N} = 7.4$ . For GaN quantum wells, this corresponds to the electron concentration  $N = 10^{12} \text{ cm}^{-2}$ . In both panels, for comparison the results at  $\mathcal{N} = 0$  are presented by the dashed lines.

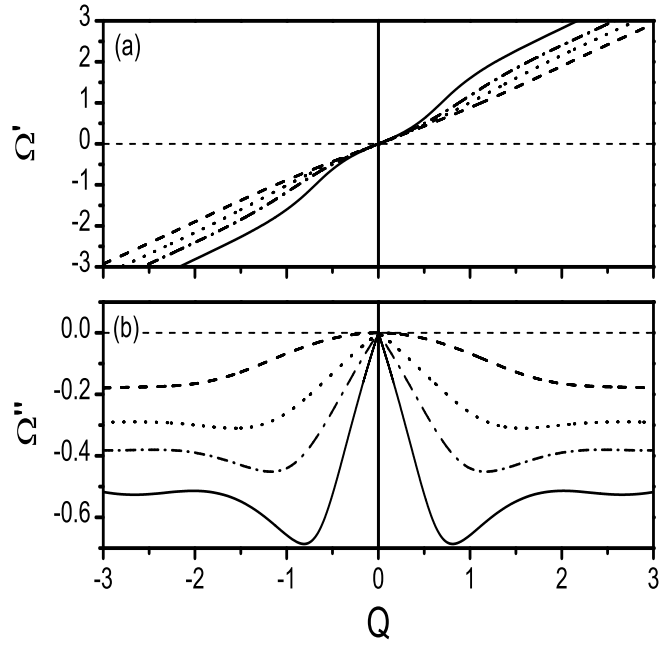


FIG. 5: The same as in Figs. 3 and 4 for the acoustic spectrum branch,  $k = 0$ , at different  $\mathcal{N}$ . For GaN quantum wells, full, dash-dotted, dotted and dashed lines correspond to  $N = 10^{12}$ ,  $5 \times 10^{11}$ ,  $2.5 \times 10^{11}$  and 0 (in  $cm^{-2}$ ).

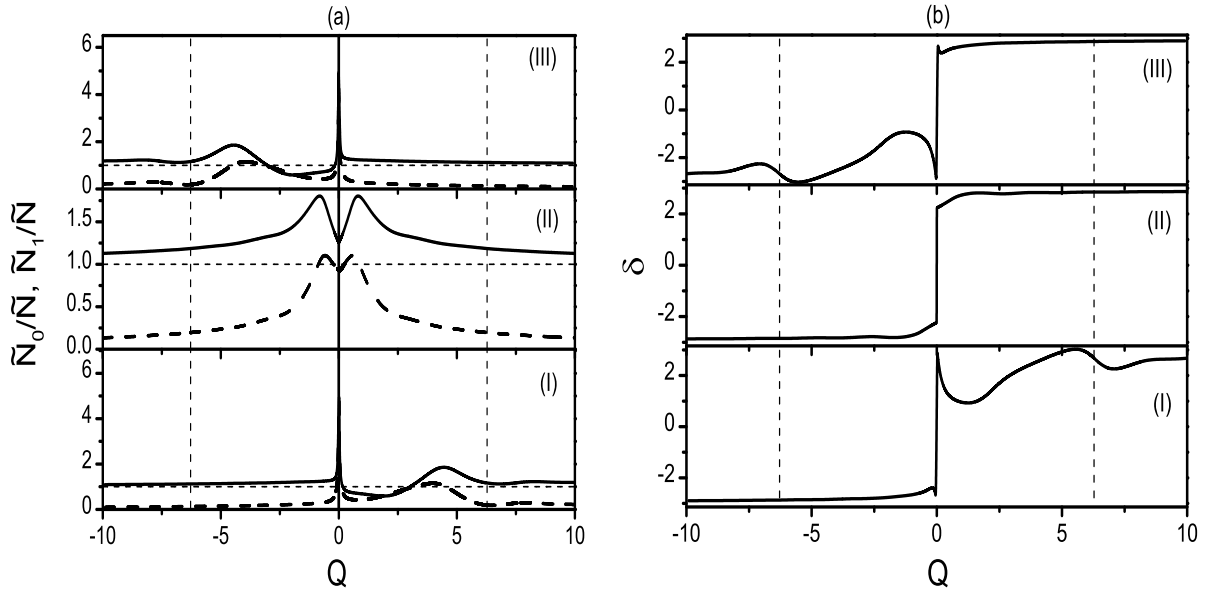


FIG. 6: Relative amplitudes and phase difference of the concentrations (see Eq. (46)) as functions of  $Q$  for three spectrum branches. Panels I, II, III, are for  $k = 1, 0, -1$ . In (a), the full and dashed lines correspond to  $\tilde{N}_1$  and  $\tilde{N}_0$ , respectively.



- 
- <sup>1</sup> W. Shockley, Bell Syst. Tech. J. Eng. **R 30**, 990 (1951).
- <sup>2</sup> Y. Katayama and K. F. Komatsubara, Phys. Rev. Lett. **19**, 1421 (1967).
- <sup>3</sup> P. F. Lu, D. C. Tsui, and H. M. Cox, Phys. Rev. Lett. **54**, 1563 (1985).
- <sup>4</sup> T. W. Hickmott, P. M. Solomon, F. F. Fang, F. Stern, R. Fischer, and H. Morkoc, Phys. Rev. Lett. **52**, 2053 (1984). L. Eaves, P. S. S. Guimaranes, B. R. Snell, D. C. Taylor and K. E. Singer, Phys. Rev. Lett. **55**, 262 (1985).
- <sup>5</sup> P. F. Lu, D. C. Tsui, and H. M. Cox, Phys. Rev. **B 35**, 9659 (1987).
- <sup>6</sup> V. Gruzinskis, P. Shiktorov, E. Starikov, L. Reggiani, L. Varani, and J. C. Vaissiere, Semicond. Sci. Technol. **19**, S173 (2004).
- <sup>7</sup> A. Iñiguez-de-la-Torre, J. Mateos, and T. Gonzalez J. Appl. Phys. **107**, 053707 (2010).
- <sup>8</sup> Gornik E and Andronov A A (ed) 1991 Opt. Quantum Electron. 23 S111360 (Special Issue on Far-infrared Semiconductor Lasers).
- <sup>9</sup> E. Starikov, P. Shiktorov, V. Gruzinskis, L. Varani, et al. J. Nanoelectron. Optoelectron **2**, 11 (2007). E. Starikov, P. Shiktorov, V. Gruzinskis, L. Varani, C. Palermo, J. F. Millithaler, and L. Reggiani, J. Phys.: Condens. Matter **20**, 384209 (2008).
- <sup>10</sup> L. E. Vorob'ev, S. N. Danilov, V. N. Tulupenko and D. F. Firsov, JETP Lett. **73**, 219 (2001).
- <sup>11</sup> V. V. Korotyeyev, V. A. Kochelap, K. W. Kim and D. L. Woolard, Appl. Phys. Lett. **82**, 2643 (2003). K. W. Kim, V. V. Korotyeyev, V. A. Kochelap, A. A.Klimov and D. L. Woolard, J. Appl. Phys. **96**, 6488 (2004).
- <sup>12</sup> J. T. Lu, J. C. Cao and S. L. Feng, Phys. Rev. **B 73**, 195326 (2006). J. T. Lu and J. C. Cao, Semicond. Sci. Technol. **20**, 829 (2005).
- <sup>13</sup> E. Starikov, P. Shiktorov, V. Gruzinskis, A. Dubinov, V. Aleshkin, L. Varani, C. Palermo, L. Reggiani, J Comput Electron (2007) **6**, 45 (2007). P. Shiktorov, E. Starikov, V. Gruzinskis, L. Varani, C. Palermo, J-F. Millithaler and L. Reggiani, Phys. Rev. **B 76**, 045333 (2007).
- <sup>14</sup> A. Akturk, N. Goldsman, G. Pennington and A. Wickenden, Phys. Rew. Lett. **98**, 166803 (2007); A. Akturk, N. Goldsman and G. Pennington, J. Appl. Phys. **102**, 073720 (2007); A. Akturk, G. Pennington, N. Goldsman, and A. Wickenden, IEEE Trans. Nanjtech. **6**, 469 (2007).
- <sup>15</sup> G. A. Baraff, Phys. Rev. **128**, 2507 (962).
- <sup>16</sup> I. I. Vosilius and I. B. Levinson, Sov. Phys. JETP **23**, 1104 (1966); **25**, 672 (1967).

- <sup>17</sup> Z. S. Gribnikov, V. A. Kochelap, Sov. Phys. JETP **31**, 562 (1970).
- <sup>18</sup> P. M. Morse, and Feshbach, H. Methods of Theoretical Physics, Part I. New York: McGraw-Hill, 1953.
- <sup>19</sup> Analyzing Eq. (40) we mentioned that there is another kind of solutions corresponding to "overdamped" excitations ( $\Omega' \sim \Omega''$ ). For them we found also a set of branches, for which  $d\Omega'/dQ < 0$ , i.e. their group velocities are negative.
- <sup>20</sup> Depending on frequency range, the space charge may lead to both additional oscillatory phenomena (plasma oscillations at high frequency collisionless electron motion) and additional relaxation (dielectric relaxation at low frequency dissipative electron motion).
- <sup>21</sup> K. Ridley, Quantum Processes in Semiconductors (Clarendon, Oxford, 1999).
- <sup>22</sup> V. V. Mitin, V. A. Kochelap, and M. A. Stroschio, Quantum Heterostructures (Cambridge University Press, New York, 1999).
- <sup>23</sup> M. J. Manfra, K. W. Baldwin, A. M. Sergent, K. W. West, R. J. Molnar and J. Caissie Appl. Phys. Lett., **85**, 5394 (2004); *ibid.*, **85**, 1723 (2004); *ibid.*, **85**, 5279 (2004).
- <sup>24</sup> C. Skierbiszewski, Z. Wasilewski, M. Siekacz, A. Feduniewicz, B. Pastuszka, I. Grzegory, M. Leszczynski, and S. Porowski, Phys. Stat. Sol. (a) **201**, 320 (2004); C. Skierbiszewski, K. Dybko, W. Knap, M. Siekacz, W. Krupczynski, G. Nowak, M. Bokowski, J. Lusakowski, Z. R. Wasilewski, D. Maude, T. Suski and S. Porowski, Appl. Phys. Lett., **86**, 102106 (2005).
- <sup>25</sup> E. A. Henriksen, S. Syed, Y. Ahmadian, M. J. Manfra, K. W. Baldwin, and A. M. Sergent, R. J. Molnar and H. L. Stormer, Appl. Phys. Lett. **86**, 252108 (2005)
- <sup>26</sup> A. Asgari, S. Babanejad and L. Faraone, J. Appl. Phys., **110**, 113713 (2011).
- <sup>27</sup> J. Falson, D. Maryenko, Y. Kozuka, A. Tsukazaki, and M. Kawasaki, Appl. Phys. Exp. **4** 091101 (2011).
- <sup>28</sup> D. G. Schlom and L. N. Pfeiffer, Nature Mater., **9** 881 (2010). A. Tsukazaki, S. Akasaka, K. Nakahara, Y. Ohno, H. Ohno, D. Maryenko, A. Ohtomo and M. Kawasaki, *ibid.*, **9**, 889 (2010).